

MSP-Former: Multi-Scale Projection Transformer for Single Image Desnowing

Sixiang Chen^{1†}, Tian Ye^{†1}, Yun Liu², Taodong Liao¹,
Yi Ye¹, and Er kang Chen^{*1}

¹School of Ocean Information Engineering, Jimei University, Xiamen, China

² Southwest University School of Artificial Intelligence, Chongqing, China

Abstract. Image restoration of snow scenes in severe weather is a difficult task. Snow images have complex degradations and are cluttered over clean images, changing the distribution of clean images. The previous methods based on CNNs are challenging to remove perfectly in restoring snow scenes due to their local inductive biases' lack of a specific global modeling ability. In this paper, we apply the vision transformer to the task of snow removal from a single image. Specifically, we propose a parallel network architecture split along the channel, performing local feature refinement and global information modeling separately. We utilize a channel shuffle operation to combine their respective strengths to enhance network performance. Second, we propose the MSP module, which utilizes multi-scale avgpool to aggregate information of different sizes and simultaneously performs multi-scale projection self-attention on multi-head self-attention to improve the representation ability of the model under different scale degradations. Finally, we design a lightweight and simple local capture module, which can refine the local capture capability of the model.

In the experimental part, we conduct extensive experiments to demonstrate the superiority of our method. We compared the previous snow removal methods on three snow scene datasets. The experimental results show that our method surpasses the state-of-the-art methods with fewer parameters and computation. We achieve substantial growth by 1.99dB and SSIM 0.03 on the CSD test dataset. On the SRRS and Snow100K datasets, we also increased PSNR by 2.47dB and 1.62dB compared with the Transweather approach and improved by 0.03 in SSIM. In the visual comparison section, our MSP-Former also achieves better visual effects than existing methods, proving the usability of our method.

1 Introduction

A series of advanced vision tasks such as object tracking [1,2], object detection [3,4] and image segmentation [5,6] in severe weather scenarios urgently require credible image restoration. Among them, snow removal from a single image

* Corresponding author. [†]Equal contribution.

is a difficult problem to overcome because multiple ill-conditioned degradations superimpose it. The imaging model of the snow scene can be modeled as this:

$$I(x) = K(x)T(x) + A(x)(1 - T(x)) \quad (1)$$

where $I(x)$ represents the snowy image, $K(x) = J(x)(1 - Z(x)R(x) + C(x)I(x)R(x))$. $K(x)$ is the veiling-free snowy image, $T(x)$ and $A(x)$ are the transmission map and atmospheric light. $C(x)$ and $I(x)$ are the chromatic aberration map for snow images and the snow mask, respectively. $J(x)$ is the snow-free image we want.

Removing snow at the earliest time is still based on a prior [7,8,9,10]. For example, Pei et al. [7] utilize the image features prior of visibility and saturation to remove snow marks. Recently, most desnowing methods have been based on convolutional neural networks(CNNs). However, the local inductive bias of CNNs leads to its lack of global modeling ability, which is essential in snow removal tasks. In HDCW-Net [11], the author uses the dual-tree wavelet transform to divide the snow scene into high and low frequencies to process the network separately, which leads to a tedious process, and it is challenging to achieve outstanding results in terms of effects.

Nowadays, with the development of the vision community, the vision transformer (Vit) has been introduced and has given people an extraordinary impression due to its powerful global modeling capabilities [12,13,14,15,16]. For example, PVT [14] enables Vit to achieve good results in high-level vision tasks by building a pyramid structure. Swin Transformer [15] caused an uproar by refreshing the optimal results of multiple advanced vision through window self-attention and window shift operations. However, the model of Vit also has its shortcomings that are hard to ignore: it lacks the ability to mine local details and requires substantial computational overhead. This leads us to think :

- *How to introduce Vit into the task of removing snow to make up for the insufficiency of CNNs’s global modeling and at the same time to balance its own shortcomings?*

From Eq.1, the degraded snow scene usually contains the snowflake, snow streak, and veiling effect. Various degradations have different size characteristics, which makes it easy to ignore some degradation information by fixing a single de-mining feature. The patch embedding operation of the Vit series makes each token have a solid receptive field and cannot capture the snow degradation of different scales simultaneously, resulting in the Vit based on global modeling also showing a particular disadvantage in repairing the degradation of different scales. This leads to our second thought:

- *How to design a lightweight and efficient network that can handle the complex degradation information in the snow scene well?*

To address the above problems, in this paper, we propose MSP-Former, a lightweight and powerful single-image snow removal network. Inspired by the powerful detail mining feature of CNNs and the global modeling capability of

Vit, we construct a channel-dimensionally parallel network architecture consisting of multi-scale projection (MSP) and local capture module (LCB) modules. The channel shuffle operation combines both advantages to improve the network’s performance. We propose a multi-scale projection self-attention for the MSP part, which adopts the average pooling of different kernels and strides to aggregate local features of different receptive fields and reduce the feature size. Furthermore, we perform multi-scale projections separately projecting to Key(**K**) and Value(**V**) for the multi-head self-attention mechanism, which improves the overall representation ability of the model with low parameters amount and computational complexity.

We show the relationship between the number of parameters of our model, the amount of computation, and the PSNR (dB) on the CSD test dataset in Fig.1. We note that our method outperforms previous SOTA methods by a large margin in all aspects. For the latest single-image snow removal network HDCW-Net, although it has an advantage in the number of parameters ($699\text{k} < 2.83\text{M}$), our approach is much lower in computation ($4.42\text{G} < 9.78\text{G}$) and much higher than it in metrics ($33.75\text{dB} > 29.06\text{dB}$, $0.96 > 0.91$). Our experiments also demonstrate that our method outperforms the performance of the model (Transweather) designed for the snow removal task in multiple severe weather conditions ($33.75\text{dB} > 31.76\text{dB}$, $0.96 > 0.93$) while maintaining the low parameter amount and computational complexity ($2.83\text{M} \ll 21.9\text{M}$).

Our overall contributions are as follows:

- a) We propose a Vit-based single image snow removal architecture, MSP-Former, which is set as two parallel branches along the channel dimension to combine the global modeling ability of Vit and the local mining ability of CNNs, respectively. We facilitate the combination of the two strengths through a channel shuffle operation.
- b) We rethink the disadvantage of Vit on the snow removal task and carefully design the MSP module, in which we use the average pooling of different kernels to aggregate local information and use multi-scale projection for multi-head self-attention to improve the representational capabilities of Vit in complex degraded environments.
- c) We conduct extensive experiments to verify our method’s superiority. The experiments demonstrate that our network outperforms the previous state-of-the-art methods on multiple snow removal datasets and is also competitive in real-world snow removal.

2 Related Works

2.1 Single Image Desnowing

Desnowing Methods Based on Prior In the early development of single-image snow removal, the image snow removal task based on deep learning has not yet emerged. Most methods make use of the prior knowledge of images to do desnow [7,8,9,10,17,18,19]. Pei *et al.* [7] exploit the image features of saturation

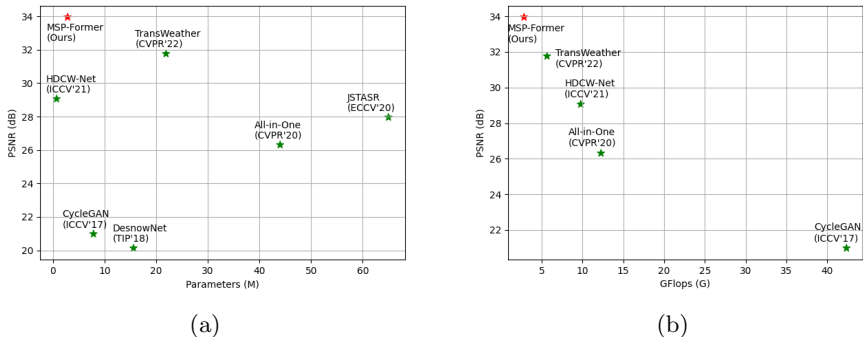


Fig. 1: (a) Trade-off between performance vs: number of parameters on CSD [11] testing dataset. The results show the superiority of our model among existing methods. (b) Trade-off between performance vs: number of operations on CSD [11] testing dataset. Multi-adds are calculated on 256×256 image. The results show the superiority of our model among existing methods.

and visibility in snow scenes to remove snow marks. Xu *et al.* utilize guidance image to recover the image from the snow scene. Affected by the difference between background edges and rain streaks, to separate snow components from the background, Zheng *et al.* [10] apply multi-guided filters to extract snow features. Wang *et al.* [8] develop a layered scheme to implement snow image decomposition and dictionary learning.

Learning-based Desnowing Methods The first learning-based method for single-image snow removal is dubbed DesnowNet [20], which sequentially handles the removal of translucent and opaque snow particles based on a multi-stage architecture resulting in huge computational overhead. After this, many deep learning methods emerged [21,11,22,23,24]. All-in-one [21] designs multiple task-based encoders that can simultaneously address various types of weather degradation. In JSTASR [22], new joint size and transparency-aware snow removal algorithm is presented, which can classify snow particles according to their size and perform snow removal at different scales. HDCW [11] applies the wavelet transform of the two-tree and proposes a hierarchical decomposition paradigm in the network to understand snow particles of different sizes better. In addition, a new feature has been contributed, called Contradictory Channels (CC) for Snowscapes. [23] proposes an asymmetric codec to handle different weather degradations while speeding up inference.

2.2 Vision Transformer

Convolutional Neural Networks(CNNs) have dominated the computer vision community for many years. In recent years, research scientists have applied

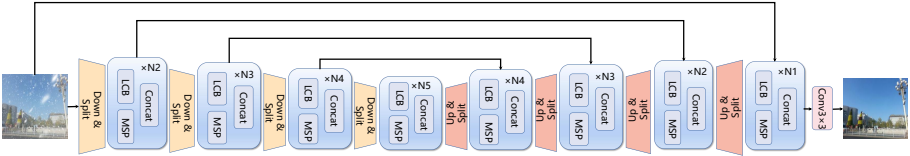


Fig. 2: Our MSP-Former consists of four stages encoder and five stages decoder, and there is a skip connection between the corresponding layers inspired by UNet [37]. We split the channel dimension at each stage and execute our LCB and MSP modules separately. After that, it is combined along the channel dimension to enter the next step. Ultimately, we use a 3×3 convolution to transform the output image.

the Transformer [25] architecture from natural language processing(NLP) to vision tasks(Vit [26]). Many excellent Vit-based works have been proposed since then [14,13,27,16,28,15,29]. PVT [14] utilizes the vision transformer in a pyramid structure and presents a spatial-reduction attention mechanism to reduce the size of key and value to reduce computational overhead. Segformer [28] used sequence reduction, which adopts linear projection to decrease computation complexity. However, despite achieving attractive results, some performance degradation is inevitable. CvT [27] proposes Convolution Token Embedding and Convolution Projection operations, which introduce convolution into Vit to improve the overall representation of the model. Benefiting from the local expression ability of convolution and the global modeling ability of Vit, Mobile-Former [29] proposes a bidirectional bridge structure of MobileNet and Transformer, which can integrate the advantages of convolution and transformer, and has low computational complexity. Swin Transformer [15] operates self-attention within the window patch and utilizes shifted window partitioning approach to construct connections between neighboring non-overlapping windows, which shows stunning results in multiple downstream tasks. Based on Swin Transformer, many following works have been proposed and used in various fields with competitive results [30,31,32,33].

Some vision transformer-based methods have also been gradually proposed for low-level tasks. Inspired by Swim Transformer, SwinIR [34] offers a model consisting of the large residual blocks based on Swin Transformer Block, which achieves non-trivial effects on many image restoration tasks. Restormer [35] proposes an MDTA module aggregating local and non-local pixel interactions while performing self-attention along the channel dimension to reduce computational cost. Uformer [36] stacks the Swin Transformer blocks into a multi-scale UNet architecture and designs a Leff module that combines the local extraction capability of depth-wise convolution(DWConv) to improve the effectiveness of the overall model. However, the single image desnowing work based on the vision transformer is not yet. Our MSP-Former proves the possibility of the transformer in the snow removal task.

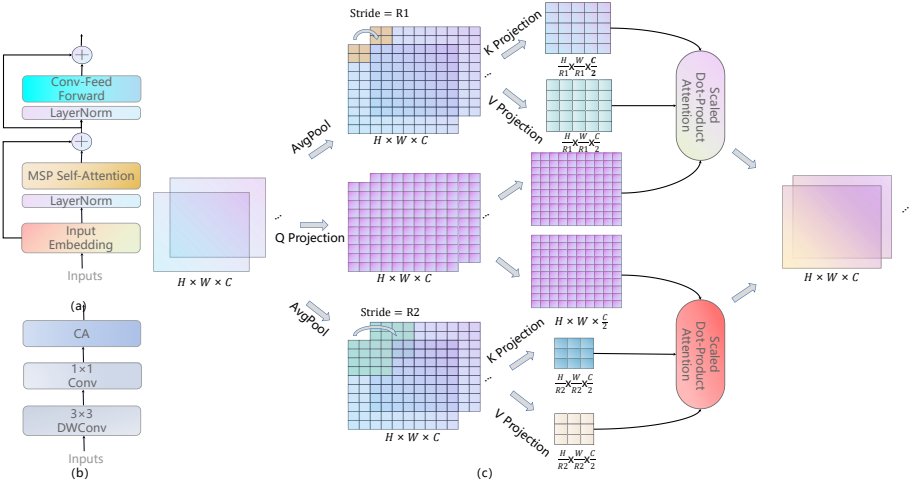


Fig. 3: (a) is the multi-scale projection(MSP) module, (b) is the local capture block(LCB) module, and (c) is the multi-scale projection self-attention mechanism(MSP Self-Attention) in the MSP module.

3 Method

3.1 Overall

An overview of the proposed MSP-Former architecture is shown in Fig.2, which is a multi-scale encoder and decoder design followed by UNet [37]. We first employ 3×3 convolutional downsampling for each stage to reduce image size and increase dimensionality. The features are split into two parts along the channel dimension and fed into our carefully designed MSP and LCB modules for global information modeling and local feature capture, respectively, which are crucial for snow removal (We perform a channel shuffle operation before each channel split, and ablation experiments prove that the channel shuffle operation can optimize our model). Afterward, we integrate the separately processed information along the channel dimension to improve the representative ability of our model on the image snow removal task. After the last decoder, we take a 3×3 to output the final snow-free map.

3.2 MSP Module

In snow images, the ill-conditioned snow degradation of different sizes overlaid on clean images makes snow removal a challenging problem. To address this issue, we elaborate on a multi-scale projection (MSP) module inspired by vanilla transformers, as shown in Fig.3.

MSP Self-Attention For the vision transformer, given an input feature $X^{H \times W \times C}$, it is usually reshaped into a 3D sequence $X_s^{N \times C}$ and a linear layer is employed to project X into Query(**Q**), Key(**K**), Value(**V**), can be expressed in the following form:

$$\text{Projection : } \mathbf{Q} = W_q X_s, \mathbf{K} = W_k X_s, \mathbf{V} = W_v X_s \quad (2)$$

where W_q, W_k, W_v are linear projection parameters. Nevertheless, due to fixed patch embedding, separate projections result in a fixed receptive field for each sequence in the global modeling after linear layer transformation. This is very disadvantageous for recovering variable degradation information in snow images.

To solve this problem, in MSP self-attention, we first use multi-scale avgpool to aggregate different local information, fully capturing additional scale information and providing multi-head self-attention with a richer global representation capability. At the same time, based on the above operations, we reduce the image size required for K and V projection to reduce the amount of self-attention computation, and we can express the aggregated features as:

$$X_1^{\frac{H}{R_1} \times \frac{W}{R_1} \times C} = \text{Avgpool}_{K_1}^{S=R_1}(X^{H \times W \times C}) \quad (3)$$

$$X_2^{\frac{H}{R_2} \times \frac{W}{R_2} \times C} = \text{Avgpool}_{K_2}^{S=R_2}(X^{H \times W \times C}) \quad (4)$$

among them, X_1 and X_2 are different feature maps, and K and S represent pooled kernel and stride. Then we use a linear layer to re-project the features that aggregate different local information to Key(**K**) and Value(**V**), respectively, for Scaled Dot-product Attention with the original Query(**Q**) to improve the multi-scale representation ability of self-attention. Inspired by multi-head self-attention [26], we divide self-attention into multiple heads, perform multi-head self-attention (MSA) separately for K(**K**) and V(**V**) with different local receptive fields, and finally concat them together. The formula can be expressed as follows:

$$\text{Multi - Scale Projection : } K_{\{1,2\}} = W_k X_{\{1,2\}}, V_{\{1,2\}} = W_v X_{\{1,2\}} \quad (5)$$

$$\text{MSA}(X) = \text{Concat}_{\{1,2\}}(\text{Softmax}\left(\frac{\mathbf{Q}_h \mathbf{K}_{h\{1,2\}}^\top}{\sqrt{D_h}}\right) \mathbf{V}_{h\{1,2\}}) \quad (6)$$

where $\{\cdot\}$ is the feature that has undergone multi-scale avgpool, h represents multi-head processing, and D_h is the dimension of each head. Considering the fine information and low-level details required in the process of self-attention, we add a depth-wise convolution before the point product of Value(**V**) to improve the local retention ability like [38] does.

MSP Transformer Block Like the vanilla Transformer, the MSP transformer block consists of two critical constructions, MSP Self-Attention and ConvFFN. It adds Laynorm before each part while adding residual connections to the MSP

Self-Attention and ConvFFN parts to stabilize the training network. The following formula can describe the entire block:

$$\begin{aligned} X' &= X + \mathbf{MSP-Self-Attention}(\mathbf{LN}(X)) \\ Y &= X' + \mathbf{ConvFFN}(\mathbf{LN}(X')) \end{aligned} \quad (7)$$

We continue to use ConvFFN [14] to replace the traditional MLP feedforward network to alleviate its shortcomings in local modeling, similar to the PVT[14] approach. It includes two FC layers to expand and compress the dimension, utilize a depth-wise convolution and GELU activation(DWConv-G) to capture local modeling features. It can be represented as:

$$Y = \mathbf{FC}(\mathbf{DWConv-G}(\mathbf{FC}(X))) \quad (8)$$

where X is the feature of the input and Y is the output feature.

3.3 LCB Module

In a single snow removal task, both the global degradation and the local degradation consisting of snow patches are included, so the local context information determines the detailed features of the restored image. Unlike the multi-scale self-attention module introduced above, we develop a local capture module parallel to the MSP module. It is worth mentioning that it differs from the complex calculation required by the transformer module. It only requires minimal computation and parameters, which plays a crucial role in the model’s performance-parameters trade-off in the snow removal task.

As illustrated in Fig.2(c), For the inputs $X^{H \times W \times C}$, we utilize 3×3 depth-wise convolution to excavate local snow features and exploit a 1×1 convolution for inter-channel interactions. In addition, the transformer is essentially self-modeling at the spatial level between patches. It lacks the modeling between channels, so we add channel attention [39] to the local capture module to increase the overall representation ability of the model. We can compute the whole LCB module as:

$$LCB(X^{H \times W \times C}) = \mathbf{CA}(\mathbf{Conv}_{K=1}(\mathbf{DWConv}_{K=3}(X^{H \times W \times C}))) \quad (9)$$

where K is the convolution kernel and CA represents channel attention. In the MSP transformer block, we use avgpool to aggregate multi-scale features, which approximates the capture of low frequencies. In contrast, in LCB, we use convolution to mine local high-frequency details, which forms complementary elements without wavelet transform similar operations in HDCW-Net [11].

3.4 Loss Function

We apply the following loss function to train our MSP-Former network.

Charbonnier Loss We introduce the Charbonnier Loss [40] as our basic reconstruction loss:

$$\mathcal{L}_{rec} = \mathcal{L}_{CR}(\mathcal{I}(X) - \mathcal{J}_{gt}). \quad (10)$$

where the \mathcal{I} is our MSP-Former network, X and \mathcal{J}_{gt} stand for input and ground-truth. \mathcal{L}_{CR} denotes the Charbonnier loss, which can be express as:

$$\mathcal{L}_{CR} = \frac{1}{N} \sum_{i=1}^N \sqrt{\|X^i - Y^i\|^2 + \epsilon^2} \quad (11)$$

where constant ϵ empirically set to $1e^{-3}$ for all our experiments.

4 Experiments

4.1 Implementation Details

Basic settings In the training details of the proposed MSP-Former, we use AdamW optimizer with the first and second momentum terms of (0.9, 0.999) and the weight decay of $5e^{-4}$ to train our framework. We set the initial learning rate to 0.0007 and employ linear decay after 250 epochs. For data augmentation, we adopt horizontal flip and random rotation by 90, 180, 270 degrees. We randomly crop a 256×256 patch as input to train 600 epochs.

Architecture Design For concise description, we illustrate our MSP-Former framework design. At each stage of the network, we set the channel dimensions to $\{32, 32, 64, 128, 256\}$ respectively, and we gradually increase the number of MSP and LCB modules to N_1, N_2, N_3, N_4, N_5 , which are set to 1, 2, 3, 4, and 6 in our network, respectively. We specify the strides R_1 and R_2 of each layer’s multi-scale average pooling as $R_1 = \{16, 16, 8, 4, 2\}$ and $R_2 = \{8, 8, 4, 2, 1\}$, the pooling kernel is also set as $K_1 = \{16, 16, 8, 4, 2\}$, $K_2 = \{8, 8, 4, 2, 1\}$. At the shallowest layer of the decoder, we also add an MSP and an LCB module to refine the original resolution image to improve the final output.

4.2 Datasets and Metrics

For a fair comparison, we adopt PSNR and SSIM to measure the performance of our model as in previous desnowing methods. We train and infer our MSP-Former on Snow100K [20], SRRS [22], and CSD [11] desnowing datasets to verify the superiority of our method. Dataset selection and testing methods follow state-of-the-art single-image snow removal methods to ensure consistent and accurate evaluations.

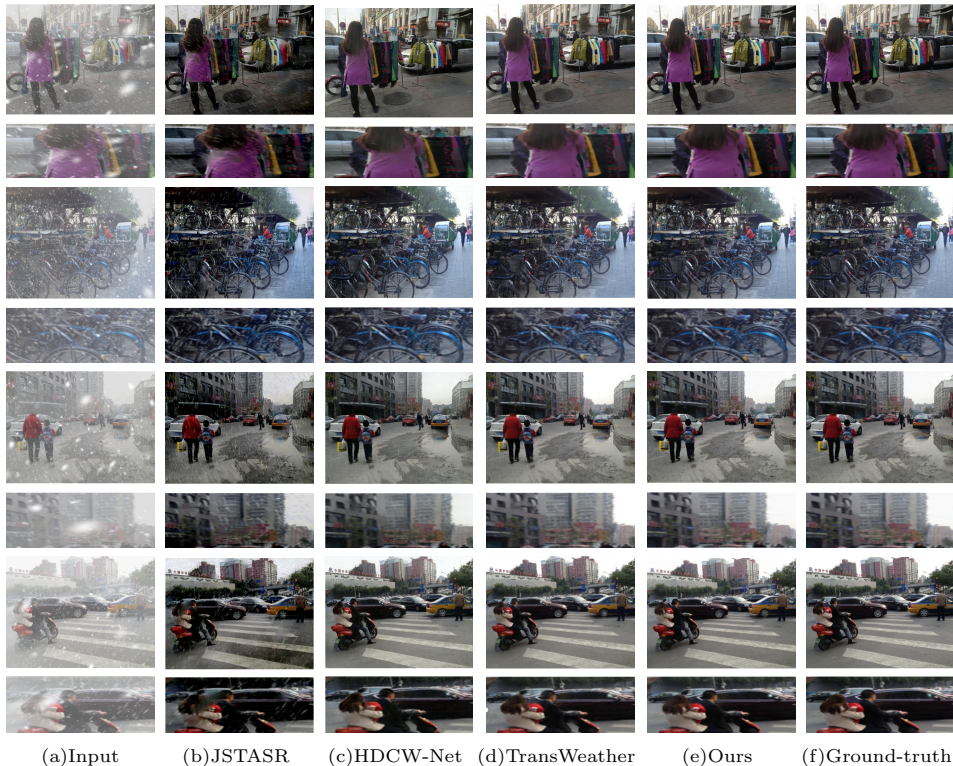


Fig. 4: Visual comparison of our method (MSP-Former) and the SOTA methods on the synthetic dataset CSD [11]. Please zoom in to see the details better.

4.3 Compare with State-of-the-art Methods

Quantitative Analysis In this section, we compare the performance of our method with other existing snow removal methods: DesnowNet [20], CycleGAN [41], All in One [21], JSTASR [22], HDCW-Net [11] and TransWeather [23]. To ensure fairness, for the methods without CSD [11] training, we re-train to meet the latest evaluation criteria of the previous single-image snow removal and take the best training results for comparison. Table 1 reports the results on different snow datasets, which shows that our model outperforms all SOTA desnowing methods. On Snow100K [20], SRRS [22] and CSD [11] testing sets, MSP-Former achieves 1.99 dB, 2.47 dB and 1.61 dB improvement on PSNR metric, and is also significantly ahead of the most advanced methods on SSIM.

Parameters and Computational Complexity Analysis For an excellent model, parameters and computation are also within the scope of measurement. The number of parameters determines whether the model is lightweight, and the

Table 1: Desnowing results on the CSD [11], SRRS [22] and Snow 100K [20] datasets (PSNR(dB)/SSIM). Underline and bold indicate the best metrics.

Method	CSD (2000) [11]		SRRS (2000) [22]		Snow 100K (2000) [20]		#Param	#GMacs
	PSNR \uparrow	SSIM \uparrow	PSNR \uparrow	SSIM \uparrow	PSNR \uparrow	SSIM \uparrow		
(TIP'18)DesnowNet [20]	20.13	0.81	20.38	0.84	30.50	0.94	15.6M	1.7KG
(CVPR'18)CycleGAN [41]	20.98	0.80	20.21	0.74	26.81	0.89	7.84M	42.38G
(CVPR'20)All in One [21]	26.31	0.87	24.98	0.88	26.07	0.88	44M	12.26G
(ECCV'20)JSTASR [22]	27.96	0.88	25.82	0.89	23.12	0.86	65M	–
(ICCV'21)HDCW-Net [11]	29.06	0.91	27.78	0.92	31.54	<u>0.95</u>	699k	9.78G
(CVPR'22)TransWeather [23]	<u>31.76</u>	<u>0.93</u>	<u>28.29</u>	<u>0.92</u>	<u>31.82</u>	0.93	21.9M	5.64G
MSP-Former	33.75	0.96	30.76	0.95	33.43	0.96	2.83M	4.42G

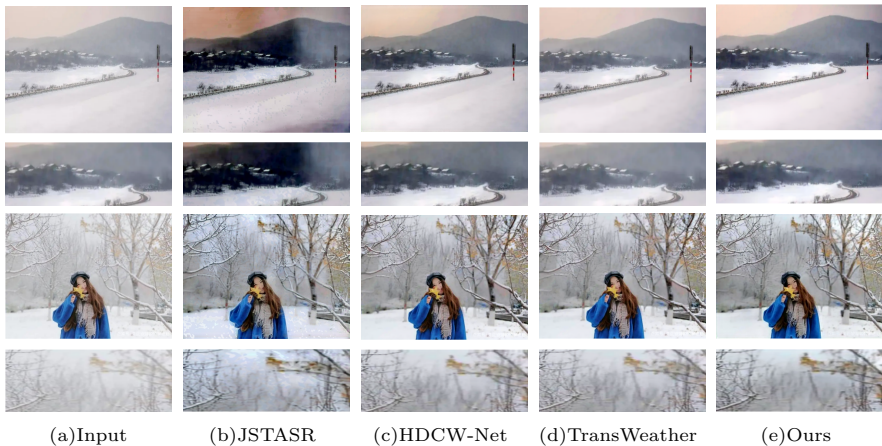


Fig. 5: Visual comparison of our method (MSP-Former) and the SOTA methods on the real-world dataset. Please zoom in to see the details better.

amount of calculation measures the model’s efficiency. We present the comparison results of computation of 256×256 size and parameters with state-of-the-art snow removal method in Table 1. We notice that our MSP-Former is better than the previous SOTA approaches in terms of both parameters and the amount of calculation, which is only 2.83M and 4.26GMacs. Although HDCW-Net [11] has only 699k parameters, we achieve advantages in computation and metrics and outperform HDCW-Net [11] in terms of performance-parameter trade-off.

Visual Comparison We compare the visual performance of MSP-Former and other state-of-the-art methods for snow removal on synthetic and real datasets, which are presented in Fig.4 and 5. It can be seen that the previous desnowing method is not able to completely remove all snow scenes at one time, especially small snow spots and snow marks. Instead, MSP-Former can remove snow degra-

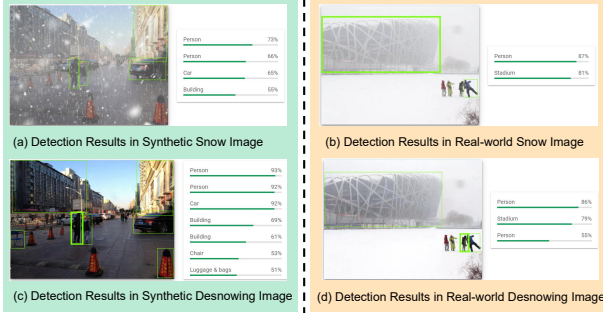


Fig. 6: On the left is the synthetic snow map and its detection confidence without snow, and on the right is the real-world snow image and its detection confidence. All confidence metrics come from the Google Vision API.

dation of various sizes very well, which is superior to previous SOTA methods in detail and background restoration. In particular, our method also attracts certain advantages in the recovery of fine snow points and overall color regions in real-world snow scenes.

4.4 Quantifiable Performance for High-level Vision Tasks

We explore the help of images before and after snow removal for high-level vision tasks, and the results are depicted in Fig.6. Our detection confidence is supported by Google Vision API. From Fig.6, it can be concluded that pictures in bad weather can affect high-level vision tasks. Our snow removal method can indirectly help the development of high-level vision tasks.

4.5 Ablation Study

In this part, we analyze the effect of each design in MSP-Former. For the ablation study, we employ the Charbonnier loss [40] as our loss function and train on the CSD [11] dataset with 256×256 for 200 epochs to test the effectiveness of our model.

Effectiveness of MSP-Self Attention To verify the effect of our avgpool local aggregate projection self-attention(AA), we replace our scheme with spatial-reduction attention(SRA) proposed by PVT [14] and max-pooling aggregate projection(MA). The results are shown in Table 2. We found that our avg-pooling local aggregation can achieve better results from its results. We think this is due to the low-frequency capture feature of avg-pooling, which can better complement another convolution branch on the snow removal task.

In addition, We also conduct multi-scale projection(MSP) and single-scale projection(SSP) ablation experiments to verify that our MSP Self-Attention can

Table 2: Comparison on CSD [11] testing dataset for our experimental configuration. Underline indicates the best metrics. (PSNR(dB)/SSIM)

Setting	Model	#Param	#GFlops	PSNR	SSIM
1	SRA	3.28M	4.61G	29.84	0.931
2	MA	2.83M	4.42G	28.57	0.903
3	AA(Ours)	2.83M	4.42G	<u>30.12</u>	<u>0.935</u>
4	SSP	2.83M	4.39G	29.49	0.921
5	MSP(Ours)	2.83M	4.42G	<u>30.12</u>	<u>0.935</u>

achieve non-trivial effects on snow removal due to its adaptation to various sizes of snow degradation information. The ablation results are also presented in Table 2.

Effectiveness of LCB Module We verify the effect of our LCB module in ablation experiments. We designed three schemes to conduct our experiments: (1) remove the LCB module (2) delete the channel attention(CA) in the LCB module (3) plus the LCB module. As described in Table 3, we observe that parallel LCB modules can boost the model’s overall recovery performance, which indicates that the model can simultaneously focus on global modeling and fine-grained recovery of local details. It is worth describing that we found that adding channel attention to the convolution module can play a vital role in the overall representational ability of the architecture with only a small amount of parameters and computation.

Table 3: Comparison on CSD [11] testing dataset for designs of our methods. Underline represents the best metrics in this table (PSNR(dB)/SSIM). w/o LCB means removing the LCB module, there is only one branch of MSP. w/o CA represents there is no channel attention mechanism in the LCB module.

Setting	Model	#Param	#GFlops	PSNR	SSIM
1	w/o LCB	2.60M	4.26G	29.21	0.919
2	LCB w/o CA	2.76M	4.42G	29.61	0.923
3	LCB(Ours)	2.83M	4.26G	<u>30.12</u>	<u>0.935</u>

Effectiveness of Channel Shuffle We remove and add channel shuffle(CS) operations respectively to observe the changes in model performance, which are

described in Table 4. The experiment proves that the information reorganization between channels brought by the channel shuffle operation can improve the effects of the network.

Table 4: Metrics comparison on CSD [11] testing dataset for channel shuffle. Underline represents the best metrics in this table (PSNR(dB)/SSIM). w/o CS represents removing the channel shuffle operation before we split the channel dimension.

Setting	Model	#Param	#GFlops	PSNR	SSIM
1	w/o CS	2.83M	4.26G	29.46	0.923
2	w CS(Ours)	2.83M	4.26G	<u>30.12</u>	<u>0.935</u>

5 Limitation

Compared to previous SOTA methods, our method is based on the transformer architecture, whose quadratic complexity constrains the speed of the model although we exploit avgpool to aggregate information while reducing the size. We put the speed comparison with the state-of-the-art method in Table 5.

Table 5: Speed comparison on CSD [11] testing dataset with 256×256 . Underline represents the best speed in this table. (PSNR(dB)/SSIM)

Setting	Model	Speed
1	TransWeather [23]	<u>0.014s</u>
2	MSP-Former	0.038s

6 Conclusion

In this paper, we propose a single-image snow removal method with a multi-scale projection transformer. Specifically, we employ average pooling to aggregate local information and combine multi-scale projections for a self-attention mechanism. On the other hand, we split the channel dimension and exploit our designed lightweight local capture module for local feature mining. The clever combination of the two can achieve state-of-the-art performance on the snow removal task

with a meager amount of parameters and computation, achieving a performance-parameters trade-off. We hope further to leverage the transformer-based model for different image restoration tasks.

References

1. Meinhardt, T., Kirillov, A., Leal-Taixe, L., Feichtenhofer, C.: Trackformer: Multi-object tracking with transformers. In: Proceedings of the IEEE/CVF Conference on Computer Vision and Pattern Recognition. (2022) 8844–8854
2. Wang, Q., Zhang, L., Bertinetto, L., Hu, W., Torr, P.H.: Fast online object tracking and segmentation: A unifying approach. In: Proceedings of the IEEE/CVF conference on Computer Vision and Pattern Recognition. (2019) 1328–1338
3. Carion, N., Massa, F., Synnaeve, G., Usunier, N., Kirillov, A., Zagoruyko, S.: End-to-end object detection with transformers. In: European conference on computer vision, Springer (2020) 213–229
4. Hu, H., Gu, J., Zhang, Z., Dai, J., Wei, Y.: Relation networks for object detection. In: Proceedings of the IEEE conference on computer vision and pattern recognition. (2018) 3588–3597
5. Chen, J., Lu, Y., Yu, Q., Luo, X., Adeli, E., Wang, Y., Lu, L., Yuille, A.L., Zhou, Y.: Transunet: Transformers make strong encoders for medical image segmentation. arXiv preprint arXiv:2102.04306 (2021)
6. Isensee, F., Jaeger, P.F., Kohl, S.A., Petersen, J., Maier-Hein, K.H.: nnu-net: a self-configuring method for deep learning-based biomedical image segmentation. *Nature methods* **18** (2021) 203–211
7. Pei, S.C., Tsai, Y.T., Lee, C.Y.: Removing rain and snow in a single image using saturation and visibility features. In: 2014 IEEE International Conference on Multimedia and Expo Workshops (ICMEW), IEEE (2014) 1–6
8. Wang, Y., Liu, S., Chen, C., Zeng, B.: A hierarchical approach for rain or snow removing in a single color image. *IEEE Transactions on Image Processing* **26** (2017) 3936–3950
9. Rajderkar, D., Mohod, P.: Removing snow from an image via image decomposition. In: 2013 IEEE International Conference ON Emerging Trends in Computing, Communication and Nanotechnology (ICECCN), IEEE (2013) 576–579
10. Zheng, X., Liao, Y., Guo, W., Fu, X., Ding, X.: Single-image-based rain and snow removal using multi-guided filter. In: International conference on neural information processing, Springer (2013) 258–265
11. Chen, W.T., Fang, H.Y., Hsieh, C.L., Tsai, C.C., Chen, I., Ding, J.J., Kuo, S.Y., et al.: All snow removed: Single image desnowing algorithm using hierarchical dual-tree complex wavelet representation and contradict channel loss. In: Proceedings of the IEEE/CVF International Conference on Computer Vision. (2021) 4196–4205
12. Graham, B., El-Nouby, A., Touvron, H., Stock, P., Joulin, A., Jégou, H., Douze, M.: Levit: a vision transformer in convnet’s clothing for faster inference. In: Proceedings of the IEEE/CVF International Conference on Computer Vision. (2021) 12259–12269
13. Chen, C.F.R., Fan, Q., Panda, R.: Crossvit: Cross-attention multi-scale vision transformer for image classification. In: Proceedings of the IEEE/CVF International Conference on Computer Vision. (2021) 357–366

14. Wang, W., Xie, E., Li, X., Fan, D.P., Song, K., Liang, D., Lu, T., Luo, P., Shao, L.: Pyramid vision transformer: A versatile backbone for dense prediction without convolutions. In: Proceedings of the IEEE/CVF International Conference on Computer Vision. (2021) 568–578
15. Liu, Z., Lin, Y., Cao, Y., Hu, H., Wei, Y., Zhang, Z., Lin, S., Guo, B.: Swin transformer: Hierarchical vision transformer using shifted windows. In: Proceedings of the IEEE/CVF International Conference on Computer Vision. (2021) 10012–10022
16. Lee, Y., Kim, J., Willette, J., Hwang, S.J.: Mpvit: Multi-path vision transformer for dense prediction. arXiv preprint arXiv:2112.11010 (2021)
17. Xu, J., Zhao, W., Liu, P., Tang, X.: Removing rain and snow in a single image using guided filter. In: 2012 IEEE International Conference on Computer Science and Automation Engineering (CSAE). Volume 2., IEEE (2012) 304–307
18. Xu, J., Zhao, W., Liu, P., Tang, X.: An improved guidance image based method to remove rain and snow in a single image. *Computer and Information Science* **5** (2012)
19. Ding, X., Chen, L., Zheng, X., Huang, Y., Zeng, D.: Single image rain and snow removal via guided l0 smoothing filter. *Multimedia Tools and Applications* **75** (2016) 2697–2712
20. Liu, Y.F., Jaw, D.W., Huang, S.C., Hwang, J.N.: Desnownet: Context-aware deep network for snow removal. *IEEE Transactions on Image Processing* **27** (2018) 3064–3073
21. Li, R., Tan, R.T., Cheong, L.F.: All in one bad weather removal using architectural search. In: Proceedings of the IEEE/CVF Conference on Computer Vision and Pattern Recognition. (2020) 3175–3185
22. Chen, W.T., Fang, H.Y., Ding, J.J., Tsai, C.C., Kuo, S.Y.: Jstasr: Joint size and transparency-aware snow removal algorithm based on modified partial convolution and veiling effect removal. In: European Conference on Computer Vision, Springer (2020) 754–770
23. Valanarasu, J.M.J., Yasarla, R., Patel, V.M.: Transweather: Transformer-based restoration of images degraded by adverse weather conditions. In: Proceedings of the IEEE/CVF Conference on Computer Vision and Pattern Recognition. (2022) 2353–2363
24. Li, Z., Zhang, J., Fang, Z., Huang, B., Jiang, X., Gao, Y., Hwang, J.N.: Single image snow removal via composition generative adversarial networks. *IEEE Access* **7** (2019) 25016–25025
25. Vaswani, A., Shazeer, N., Parmar, N., Uszkoreit, J., Jones, L., Gomez, A.N., Kaiser, Ł., Polosukhin, I.: Attention is all you need. *Advances in neural information processing systems* **30** (2017)
26. Dosovitskiy, A., Beyer, L., Kolesnikov, A., Weissenborn, D., Zhai, X., Unterthiner, T., Dehghani, M., Minderer, M., Heigold, G., Gelly, S., et al.: An image is worth 16x16 words: Transformers for image recognition at scale. arXiv preprint arXiv:2010.11929 (2020)
27. Wu, H., Xiao, B., Codella, N., Liu, M., Dai, X., Yuan, L., Zhang, L.: Cvt: Introducing convolutions to vision transformers. In: Proceedings of the IEEE/CVF International Conference on Computer Vision. (2021) 22–31
28. Xie, E., Wang, W., Yu, Z., Anandkumar, A., Alvarez, J.M., Luo, P.: Segformer: Simple and efficient design for semantic segmentation with transformers. *Advances in Neural Information Processing Systems* **34** (2021)

29. Chen, Y., Dai, X., Chen, D., Liu, M., Dong, X., Yuan, L., Liu, Z.: Mobile-former: Bridging mobilenet and transformer. In: Proceedings of the IEEE/CVF Conference on Computer Vision and Pattern Recognition. (2022) 5270–5279
30. Liu, Z., Ning, J., Cao, Y., Wei, Y., Zhang, Z., Lin, S., Hu, H.: Video swin transformer. In: Proceedings of the IEEE/CVF Conference on Computer Vision and Pattern Recognition. (2022) 3202–3211
31. Liu, Z., Hu, H., Lin, Y., Yao, Z., Xie, Z., Wei, Y., Ning, J., Cao, Y., Zhang, Z., Dong, L., et al.: Swin transformer v2: Scaling up capacity and resolution. In: Proceedings of the IEEE/CVF Conference on Computer Vision and Pattern Recognition. (2022) 12009–12019
32. Cao, H., Wang, Y., Chen, J., Jiang, D., Zhang, X., Tian, Q., Wang, M.: Swin-unet: Unet-like pure transformer for medical image segmentation. arXiv preprint arXiv:2105.05537 (2021)
33. Tang, Y., Yang, D., Li, W., Roth, H.R., Landman, B., Xu, D., Nath, V., Hatamizadeh, A.: Self-supervised pre-training of swin transformers for 3d medical image analysis. In: Proceedings of the IEEE/CVF Conference on Computer Vision and Pattern Recognition. (2022) 20730–20740
34. Liang, J., Cao, J., Sun, G., Zhang, K., Van Gool, L., Timofte, R.: Swinir: Image restoration using swin transformer. In: Proceedings of the IEEE/CVF International Conference on Computer Vision. (2021) 1833–1844
35. Zamir, S.W., Arora, A., Khan, S., Hayat, M., Khan, F.S., Yang, M.H.: Restormer: Efficient transformer for high-resolution image restoration. In: Proceedings of the IEEE/CVF Conference on Computer Vision and Pattern Recognition. (2022) 5728–5739
36. Wang, Z., Cun, X., Bao, J., Zhou, W., Liu, J., Li, H.: Uformer: A general u-shaped transformer for image restoration. In: Proceedings of the IEEE/CVF Conference on Computer Vision and Pattern Recognition. (2022) 17683–17693
37. Ronneberger, O., Fischer, P., Brox, T.: U-net: Convolutional networks for biomedical image segmentation. In: International Conference on Medical image computing and computer-assisted intervention, Springer (2015) 234–241
38. Ren, S., Zhou, D., He, S., Feng, J., Wang, X.: Shunted self-attention via multi-scale token aggregation. In: Proceedings of the IEEE/CVF Conference on Computer Vision and Pattern Recognition. (2022) 10853–10862
39. Hu, J., Shen, L., Sun, G.: Squeeze-and-excitation networks. In: Proceedings of the IEEE conference on computer vision and pattern recognition. (2018) 7132–7141
40. Charbonnier, P., Blanc-Feraud, L., Aubert, G., Barlaud, M.: Two deterministic half-quadratic regularization algorithms for computed imaging. In: Proceedings of 1st International Conference on Image Processing. Volume 2., IEEE (1994) 168–172
41. Engin, D., Genç, A., Kemal Ekenel, H.: Cycle-dehaze: Enhanced cyclegan for single image dehazing. In: Proceedings of the IEEE conference on computer vision and pattern recognition workshops. (2018) 825–833